

RESOLUTION IMPROVEMENT FOR COMPOUND EYE IMAGES THROUGH LENS DIVERSITY

Sally L. Wood¹ Dinesh Rajan² Marc P. Christensen² Scott C. Douglas² Bonnie J. Smithson¹

¹Department of Electrical Engineering
Santa Clara University
Santa Clara, California, 95053 USA

²Department of Electrical Engineering
Southern Methodist University
Dallas, Texas, 75275 USA

ABSTRACT

Reconstruction of high resolution images from multiple low resolution images at various displacements is a well studied, ill posed problem. Designs using lenses with different imaging characteristics improve the theoretical results and also reduce the image reconstruction problem to a set of loosely coupled smaller reconstructions. This paper derives the performance limits for reconstruction from multiple lower resolution images as a function of measurement bit precision and measurement noise.

1. INTRODUCTION

A traditional digital optical imaging device collects an image using a single lens and digitizes the resulting image field using a detector array. The bulk of the cost associated with this approach is usually in the optical elements, and the length requirements of the optical column preclude the use of a flat form factor for the device. This method of image formation is markedly different from that used in radio astronomy or medical imaging, where the image field is sampled using lower-quality elements and image reconstruction methods are used to compute better quality images. Recent advances in optical imaging sensors have created an opportunity to bridge these two imaging approaches to achieve devices with a flat form factor. Flat cameras have potential applications ranging from conformal sensing skins on surveillance aircraft to head-mounted camera patches for firemen and rescue workers..

The TOMBO imaging device [4] is an example of such a system that uses an array of small lenses and sensors to create a corresponding array of overlapping low-resolution images which are recombined to form a higher-resolution image. This type of reconstruction task is similar to that of computed tomography in medical imaging [3], as well as the motion-blur problem [e.g. 1].

Reconstruction of high resolution images from multiple overlapping low resolution images is a well-known super-resolution problem [2]. The resolution of the reconstruction will depend on how many different low resolution images are available and the amount of relative translation. Small amounts of translation are needed for high resolution, but small translations also result in a small amount of new information from each additional image. The best results are obtained when the translations of the low resolution images are precisely known, the bit precision of the observed pixel values is very high, the blurring function is known, and the measurement noise is at a minimum. The quantization limits of the measurements will contribute to the measurement noise. The objective is to develop computationally-efficient procedures for high-quality image reconstruction.

Advances in sensor and processing technology have enabled a variety of novel flat camera designs employing multiple image sensors to be developed. In this paper, we study the problem of reconstructing high resolution images from multiple low resolution images in this context, and develop an optimal estimator. Performance of the reconstruction algorithm can be improved and made more robust by adding observations taken from sensor/lens systems with different magnifications. The solution with multiple lens magnifications is shown to lead to a modular reconstruction method that allows small loosely coupled subtiles to be estimated separately. This reduces the complexity of using the estimator. The role of diversity in obtaining high resolution reconstructed images in this formulation can be extended to allow us to strategically add new measurements. The technique allows for parallel computation and merging of multiple reconstruction results. Computations of expected error and an image reconstruction example demonstrate the advantages of our approach.

In this paper we first describe the imaging system model and introduce notation for the observations from overlapping subarrays of low resolution pixels.

Performance for the initial system and the improved system is compared, and a general methodology for designing an optimally improved system with limited resources is introduced. Finally performance under different measurement noise conditions and computational issues are explored.

2. IMAGING SYSTEM MODEL

For traditional single lens high resolution imaging, the observed image \mathbf{g} is related to the desired image \mathbf{f} by an observation matrix \mathbf{H} as

$$\mathbf{g} = \mathbf{H} \mathbf{f} + \mathbf{v}. \quad (1)$$

The two dimensional images are stored in the vectors \mathbf{f} and \mathbf{g} in row order, and vector \mathbf{v} represents the measurement noise. The recovery of the desired image \mathbf{f} from the observed image \mathbf{g} is a problem of image restoration based on knowledge of a deterministic \mathbf{H} , the statistics of the noise, and the image class from which \mathbf{f} was taken. Ideally, \mathbf{H} is very close to the identity matrix, but in practice the blurring in the optics makes \mathbf{H} different from the identity matrix.

When multiple small images formed with multiple small lenses are used to create an estimate of the desired image, it can be considered a problem of image reconstruction, because new observations can be used to add new information about \mathbf{f} . Consider a small $P \times P$ pixel image sensor array with a small lens that causes each pixel of the sensor to average an $M \times M$ array of pixels at the desired resolution of \mathbf{f} . With only that observation, some restoration of \mathbf{f} might be possible, but little improvement could be expected. However, if an imaging unit with an $M \times M$ array of small $P \times P$ pixel subarrays with the same geometry is used to provide images that are offset by amounts equal to the desired resolution of \mathbf{f} , then these low resolution images can be combined to compute a higher resolution reconstruction.

A device that would capture the small images was demonstrated in [4]. It used a standard image sensor array divided into smaller subarrays with separate lenses. Although the range of the device was limited because all subarrays had parallel view-plane normals, the authors point out that inserting prismlets would allow the desired overlap at any range. A similar imaging geometry is illustrated in Figure 1. A slice through one unit of the imaging system is shown schematically with the desired pixels in \mathbf{f} shown at the top and the observed pixels from the low resolution observations, \mathbf{g} , shown at the bottom. Each low resolution pixel is an average of 5 of the desired pixels. The fields of view of the subarrays, with 7 pixels

each, are offset by one pixel spacing at the desired resolution of \mathbf{f} .

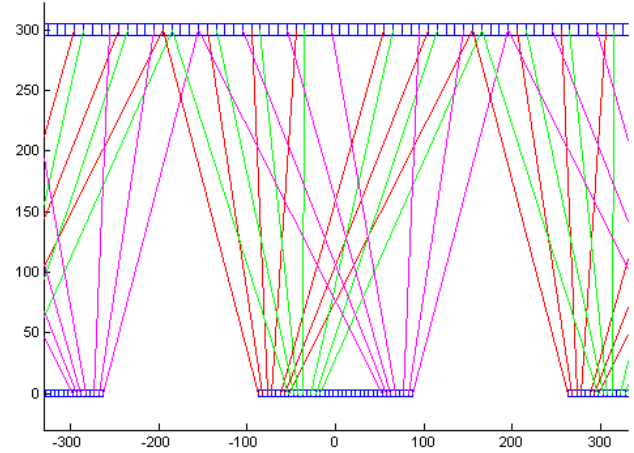


Figure 1: Overlapping subarray fields of view.

If there is a separable weighting of the contributions of the pixels in the $M \times M$ square of desired image pixels to each observed subarray pixel, then the reconstruction also can be computed separably, i.e., processing can first be done along rows and then along the columns. Separability is not necessary for reconstruction, but the mathematical notation for the separable case will be simpler. Let the vector $\mathbf{f} = [f(0) f(1) \dots f(N-1)]^t$ represent one row of the desired image. The values of pixels in the first subarray, \mathbf{g}_0 are given by

$$\mathbf{g}_0 = [g_0(0) \ g_0(1) \ g_0(2) \ \dots \ g_0(P-1)]^t \quad (2)$$

$$= [\mathbf{h}\mathbf{f} \ \mathbf{h}\mathbf{Z}^M\mathbf{f} \ \mathbf{h}\mathbf{Z}^{2M}\mathbf{f} \ \dots \ \mathbf{h}\mathbf{Z}^{(P-1)M}\mathbf{f}]^t \quad (3)$$

where \mathbf{h} is a row vector with M adjacent nonzero elements and \mathbf{Z} is a shift matrix which shifts the elements of the row vector one element to the right. The next subarray, \mathbf{g}_1 , will be positioned so that $\mathbf{g}_1(0) = \mathbf{h}\mathbf{Z}\mathbf{f}$ and in general pixel q of subarray k will be $\mathbf{g}_k(q) = \mathbf{h}\mathbf{Z}^{(qM+k)}\mathbf{f}$. The observations can be arranged in a vector sorted by the exponent of the shift vector so that M subarrays of P pixels each form a vector \mathbf{g} of length MP , and \mathbf{H} in (1) is a Toeplitz matrix.

A linear minimum variance of error estimate for \mathbf{f} for any arbitrary \mathbf{H} can be computed as

$$\hat{\mathbf{f}} = \mathbf{f}_0 + \mathbf{R}_0 \mathbf{H}^t (\mathbf{H} \mathbf{R}_0 \mathbf{H}^t + \mathbf{R}_v)^{-1} (\mathbf{g} - \mathbf{H} \mathbf{f}_0) \quad (4)$$

$$= \mathbf{f}_0 + \mathbf{A} (\mathbf{g} - \mathbf{H} \mathbf{f}_0),$$

where \mathbf{f}_0 is the expected average value for the image, \mathbf{R}_v is the covariance matrix for the noise vector \mathbf{v} , and \mathbf{R}_0 is the covariance matrix for the initial estimate of the image data. With the specific structure of \mathbf{H} described earlier, efficient computational methods for sparse Toeplitz matrices can be used. Deconvolving the blur is a poorly conditioned operation, and it is important that the estimate

of \mathbf{R}_v , be reasonable for the actual measurement noise expected. The number of bits used to represent the observations can be selected so that the quantization noise is significantly smaller than the measurement noise. If the values in \mathbf{R}_v are underestimated, the reconstructed image will have too much added noise, and if the values in \mathbf{R}_v are overestimated, the reconstructed image will not have as much of the blur removed.

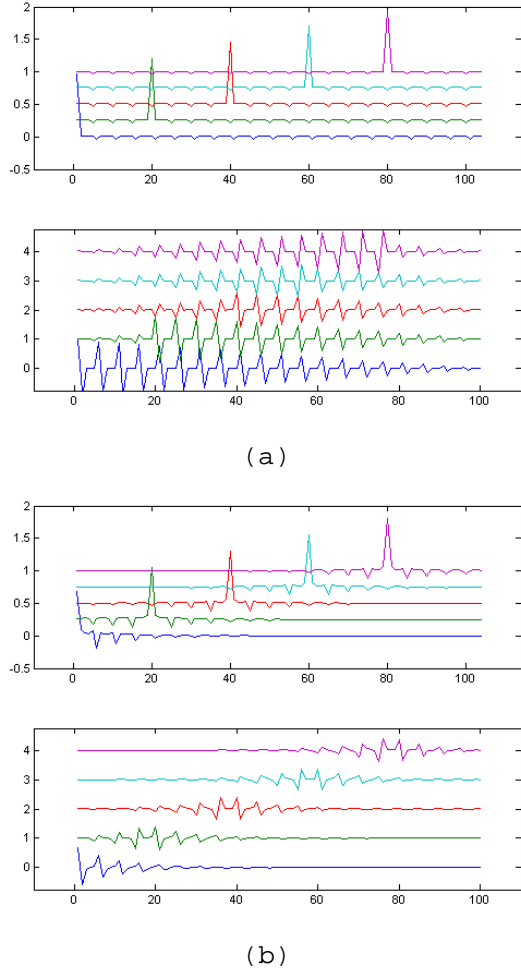


Figure 2: Graphs for selected pixels of the relative contribution of all original image pixels (upper plots) and the reconstruction filter coefficients for the low resolution image pixels (lower plots). In (a) the estimator was designed for an expected noise variance of 10^{-6} while in (b) the estimator was designed for an expected noise variance of 10^{-1} .

Figure 2 graphically shows the contribution of original image pixels to the estimate rows of \mathbf{AH} , for the selected pixels and shows the reconstruction filters, rows of \mathbf{A} , for the same pixels. Three adjacent imaging units, each with $M=5$ and $P=7$ were simulated. In Figure 2a the diagonal elements of \mathbf{R}_v were estimated to be 10^{-6} while in Figure 2b the diagonal elements of \mathbf{R}_v were estimated to be 10^{-1} . When the measurement noise is assumed to be low, a

large number of the 105 observations make a significant contribution to each estimate of a desired pixel, which would cause significant degradation in the case of high measurement noise. The estimated pixel values have little correlation with other original image pixels in this low noise environment. When the measurement noise is assumed to be higher, the reconstruction filters are more localized, so measurement errors can not propagate as far as they could in the low noise estimate case. However, the high noise estimate causes a higher correlation of a pixel estimate with other pixels in the image.

3. DIVERSITY IN IMAGE BLUR

The performance of the image pixel estimator can be improved by taking additional measurements. A second set of measurement taken with the same sensor arrays will effectively produce a single set of measurements with reduced noise due to averaging. However, if a different imaging geometry is used for the second set of measurements, there will be much greater improvement in the reconstructed image. For example, Figure 3 shows the same type of information shown in Figure 2 for an imaging system with two overlapping sets of subarrays. The first set has $M_1=5$ and $P_1=7$ and the second has $M_2=7$ and $P_2=5$. The size of M would be determined by constraints on the lens size but other lenses with similar values could be manufactured within the same constraints. For both noise levels the reconstruction filter is relatively localized to the appropriate observations from each set of subarrays.

The performance of the reconstruction filters can be compared by computing the expected mean squared error of the reconstructed image for different filters. In Figure 4, the expected errors are plotted as a function of actual noise variance for estimators which assumed a noise variance of 10^{-4} and 10^{-2} . Three different imaging geometries are compared. The two curves marked with circles use one imaging unit with $M=5$ and $P=7$. In the curves marked with an "x", two sets of measurements were taken of the same area with the same imaging unit. These curves have a lower expected error, which is most noticeable at the higher actual noise levels, due to averaging. The third geometry uses two overlapping imaging units, one with $M=5$ and $P=7$ and a second unit viewing the same area with $M=7$ and $P=5$. These curves, marked with triangles, show superior performance due to the diversity in the image blur and will form much sharper images under low noise conditions. For the higher values of actual noise variance the expected error is lower for the estimator based on the higher expected noise variance, although the differences are not noticeable using the plotting scales shown.

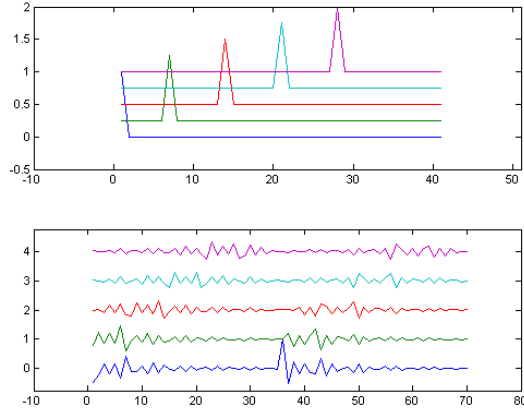


Figure 3: Graphs of reconstruction filter coefficients for overlapping sets of subarrays with $M=5$ and $M=7$ at selected pixels. The contributions to the image estimate of original image pixels are also shown. The estimated noise variance is 10^{-6} . Here the first set of subarrays has $M_1=5$ and $P_1=7$ and the second has $M_2=7$ and $P_2=5$.

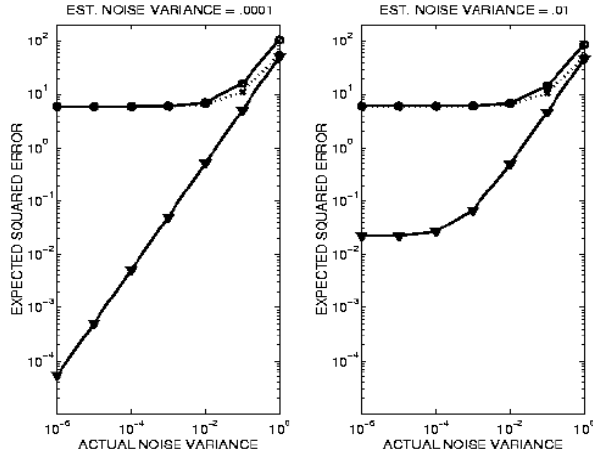


Figure 4: Expected error as a function of actual noise variance for several imaging geometries and reconstruction filters.

4. GENERAL IMAGING SYSTEM DESIGN

The improvement in reconstruction quality gained by using images with different amounts of blur suggests that a more general formulation of the problem would result in the optimal design of an imaging system composed of multiple low resolution imaging units. To allow different parts of the image to have different error tolerances, a weighting matrix \mathbf{W} is introduced. The general design problem can be formulated as

$$\min_{H \in \mathcal{H}} \min (Wf - W\hat{f})^T (Wf - W\hat{f}), \quad (5)$$

where \mathbf{W} is a weighting factor that weights different portions of the image based on *a priori* data. Other possible objective functions could also be used, such as the p -norm of the reconstruction error. The set of allowed observation matrices \mathcal{H} can be constrained based on the physical properties of the imaging system. For example, a simple constraint ensures that all rows of \mathbf{H} have finite energy. The minimization in (5) is both over the set of all observation matrices \mathcal{H} and also over all possible reconstruction strategies. In this generalized form, computing a solution to the optimization problem is difficult. A simplification is obtained if the estimation technique is fixed, like for example, the minimum variance of error estimator (4). Iterative methods can also be used to solve (5), i.e., based on a given \mathbf{H} matrix, we can compute the best reconstruction and then using this reconstruction a better \mathbf{H} can be computed.

4.1. Strategic addition of new measurements

Also, even if a desirable observation matrix \mathbf{H} exists, the physical optical properties may not allow manufacturing of lenses with the desired responses. In this paper, we present results for a particular class of \mathcal{H} . In particular, we allow \mathcal{H} to be all matrices of the

form $\begin{bmatrix} H_0 \\ \tilde{h} \end{bmatrix}^T$, where H_0 is a given observation matrix

and $\tilde{h} = h_0 \mathbf{Z}^x$. Recall that \mathbf{Z} is a shift matrix that shifts the elements of the row vector one element to the right. The only allowed variable is the amount of rotation of the last row of the observable matrix, which is denoted by x . This approach can be extended to compute what new measurements will most improve an image estimate.

Thus the optimization problem reduces to

$$\min_{H \in \mathcal{H}} (Wf - W\hat{f})^T (Wf - W\hat{f}), \quad (6)$$

where \hat{f} is as defined in (4). This optimization problem is solved numerically. A sample result of the optimization is given in Figure 6. For this example, the weighting matrix had large values for pixels 6-11 and the size of the reconstruction filter used in the last row of H was 8. Clearly, the optimization puts the filter around pixels with larger weight.

4.2. Examples with a real image

The reconstructed images with and without diversity in the observations are given in Figure 5a and Figure 5b

respectively. In Figure 5a, filter blurs of sizes $M=5$ and $M=7$ were used, whereas in Figure 5b only filters of size $M=5$ were used.

Using diversity in the image blur resulted in an increase in PSNR from 27.5dB to 31.0dB for this particular image. The sharpness of the image in Figure 5a is evident. It should be noted that the number of observations in both cases is maintained constant. We are currently researching methods to characterize the variation in the blurs between the different filters that results in maximal gains.

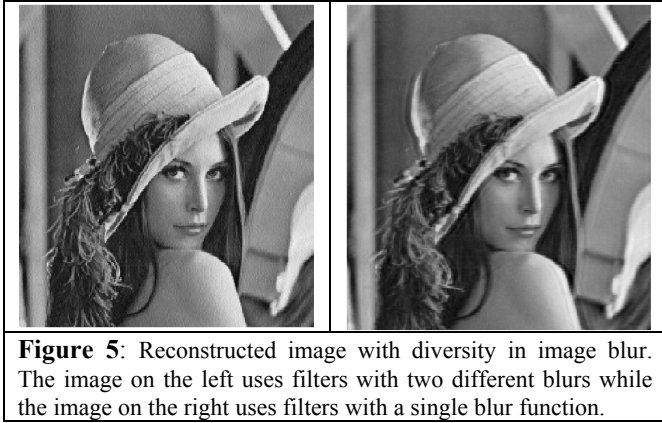


Figure 5: Reconstructed image with diversity in image blur. The image on the left uses filters with two different blurs while the image on the right uses filters with a single blur function.

5. COMPUTATION WITH LOW RANK UPDATES

When adjacent imaging units are used to expand the field of view of the image, each unit can independently compute the reconstruction of the area it views. However there will be some overlap, and the results from the separate units can be combined to for an improved reconstruction. This can also be done by forming a single observation matrix, where the nonzero elements are close to the main diagonal even when the structure is not exactly Toeplitz. Using (4), define $R_e = (HR_0H' + R_v)$, and then R_e will be of the form

$$R_e = \begin{bmatrix} C & D \\ D' & C \end{bmatrix}, \quad (7)$$

The off diagonal block, D , will have very low rank of the order of M . Rather than compute the total image estimate from the larger matrix of Equation (7), the two independent reconstructions of much lower computational complexity can be combined with a low rank update to include the coupling indicated by D .

6. CONCLUSIONS

In this paper, we presented computationally simple reconstruction methods for an imaging system based on the compound eye approach. We also formulated a general optimization framework for the design of optimal blurring filters and provided solutions in one simple scenario. This framework for designing optimal blur filters can be specialized to different scenarios of interest. For example, filters with a certain roll-off factor but variable bandwidth can be parameterized and optimal bandwidth calculated for the imaging system of interest.

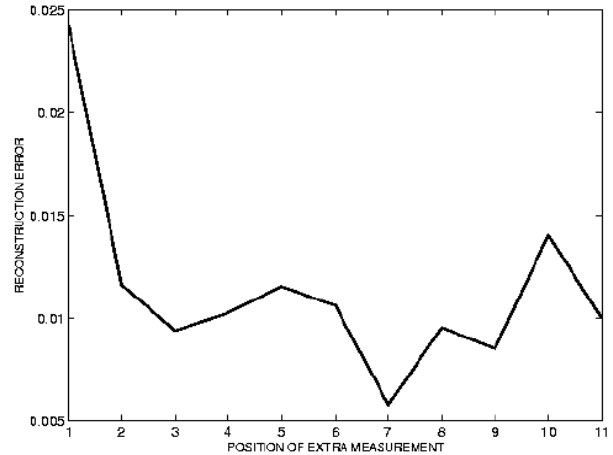


Figure 6: Plot of reconstruction error for various positions of the extra measurement.

7. REFERENCES

- [1] L. G. Brown, "A Survey of Image Restoration Techniques," *ACM Computing Surveys*, vol. 24, no.4, pp325-376, December 1992.
- [2] S. Chaudhuri, ed. *Super-Resolution Imaging*, Kluwer Academic Publishers, Boston MA, 2001.
- [3] A. Macovski, *Medical Imaging Systems*, Prentice Hall, Englewood Cliffs, N.J., 1983.
- [4] J. Tanida, T. Kumagai, K. Yamada, S. Miyatake, K. Ishida, T. Morimoto, N. Kondou, D. Miyazaki, Y. Ichioka, "Thin Observation Module by Bound Optics (TOMBO): Concept and experimental verification," *Appl. Optics-IP*, vol. 40, no. 11, p. 1806, Apr. 2001.